Central European Journal of Energetic Materials, **2015**, *12*(4), 623-635
ISSN 1733-7178
e-ISSN 2353-1843

Research on the Influence of Charge Diameter upon the Output Pressure of Small-Sized Explosives

Bingliang BAO*, Nan YAN, Feng ZHU

State Key Laboratory of Explosion Science and Technology,
Beijing Institute of Technology,
5 South Zhongguancun Street, Haidian District, Beijing, China
** E-mail: bbl793608087@gmail.com*

Abstract: By combining experimental tests and numerical simulations, the output pressure of JO-9c explosive was measured for a series of small-sized charge diameters, and qualitative rules and a quantitative model were obtained for the influence of charge diameters upon the JO-9c explosive output pressure. Results show that a small-sized charge diameter has a significant influence on the output pressure; in addition, the closer the charge diameter gets to the JO-9c critical diameter, the greater is the effect. The limiting diameter of JO-9c is 5 mm, and the critical diameter is approximately 0.34 mm. The deviation between numerical simulation results and experimental values shows that the numerical simulation method can predict detonation pressure with 15% uncertainty in the study of detonation rules for small-sized charges.

Keywords: manganin piezo-resistance test method, numerical simulation, output pressure, charge diameter

1 Introduction

With Micro-Electro-Mechanical System (MEMS) technology development and its application in weapon systems, the size of the pyrotechnic charges has been greatly restricted [1, 2]. This demands further miniaturized internal charges, and issues a challenge for reliable transmission of xplosive detonation, ranging from the critical diameter to the limiting diameter. Furthermore, the output pressure of a small-sized explosive is an essential parameter for measuring its initiating capacity and is of great significance to the design of the explosive train. Due

to the non-ideal detonation developed by small-sized charges, the theoretically calculated values deviate significantly from the detonation pressure of small-sized explosives; therefore, it is quite necessary to measure the detonation pressure of small-sized charges by both experiment and numerical simulation.

Much previous work has been done on the explosives' critical diameter and limiting diameter, are mainly focused on the detonation velocity test to obtain the diameter effect [3-5]. In order to obtain the range of output pressure generated by small-sized charges from the critical diameter to the limiting diameter, self-designed miniature manganin piezo-resistive sensors were used in the experiments, together with AUTODYN software for the numerical simulations. The detonation output pressure with small-sized charges was accurately measured, and the influence rules for the effect of small charge diameter on the output pressure was reliably obtained, providing researchers with valuable reference information.

2 Experimental

In the manganin piezo-resistance test method, a constant current source is used to provide the rated current I for the sensor. When the sensor is subjected to the outside pressure, the resistance and voltage changes satisfy the formula as follows:

$$\frac{\Delta R}{R_0} = \frac{I\Delta R}{IR_0} = \frac{\Delta V}{V_0}$$

where $\Delta R/R_0$ is the resistance change rate of the manganin piezo-resistive sensor, and $\Delta V/V_0$ is the voltage change rate that corresponds to the resistance change. Once the voltage change has been accurately measured, the actual (measured) pressure value can be calculated from the relationship of the voltage and pressure, which has been previously calibrated.

The connection diagram of the test system is shown in Figure 1. This test system is composed of the following sections: high-speed sync pulse constant current source, small explosive containers, digital storage oscilloscope, detonator, explosive pellet under test, organic glass protective sheet, organic glass pressure block and H manganin piezo-resistive sensors. The electric detonator was enclosed by a 45# steel sleeve, and small-sized explosive charges were used to reduce the lateral rarefaction effect as much as possible and to improve the

quality of assembly and positoning.

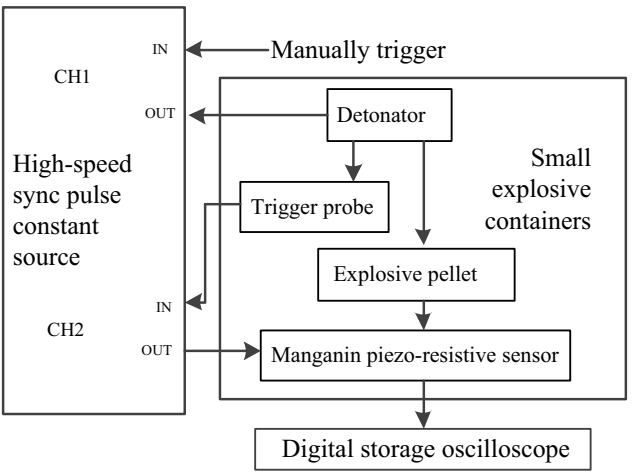

Figure 1. The connection diagram of the test system.

Unlike other previous test systems, an 8# detonator can extend the whole test time of the experiment because of its long function time. To reduce the sensor conduction time, a trigger probe was applied to the system to initiate a channel of constant current and to generate the sensor power supply.

The basic test process was as follows: the electric detonator was triggered manually, and the detonation products generated by the electric detonator were conducted to the probes. A constant current source was triggered to generate the sensor power supply. After the electric detonator initiated the small-sized charge, the detonation pressure passed through a 1 mm-thick organic glass protective sheet onto the miniature manganin piezo-resistive sensor, during which time the resistance change was collected by the test system, and the voltage change was recorded by the storage oscilloscope. Finally the measured values of the voltage change ΔV and the reference voltage V_0 were substituted into the manganin piezo-resistive sensor calibration formula to obtain the corresponding shock wave peak pressure.

The calibration curve of the H manganin piezo-resistive sensor was as follows:

$$\begin{cases} P = 53.22 \times \dfrac{\Delta R}{R} & (0 \sim 5.907 \text{ GPa}) \\ P = 1.978 + 35.28 \times \dfrac{\Delta R}{R} & (\geq 5.907 \text{ GPa}) \end{cases} \tag{1}$$

where $\frac{\Delta R}{R}$ is the resistance change rate of the manganin piezo-resistive sensor, and P is the pressure applied to the manganin piezo-resistive sensor, GPa.

Because there is a 1-mm-thick organic glass protective sheet at the top of the sensor, the pressure obtained from the sensor should be corrected according to the attenuation formula of a shock wave in PMMA [6]:

$$\begin{cases} P_{mx} = P_{m0} e^{-\alpha x} \\ \alpha = 0.0906 + 0.8615 e^{-\left(\frac{d}{2.1743}\right)} \end{cases} \tag{2}$$

In this formula, P_{m0} is the initial incident pressure of the shock wave on the organic glass, GPa; P_{mx} is the shock wave pressure on the organic glass at a distance x from the plane of incidence, GPa, α is the shock wave attenuation coefficient in the organic glass, d is the charge diameter, mm.

For small-sized explosives, the major factors that affect detonation pressure are: explosive type, charge diameter, charge density, charge height, *etc*. When designing the experimental programme, given full consideration to the applications of small-sized detonating tubes as reported in the literatures, JO-9c was chosen as the experimental explosive, which is based on HMX (95%HMX/5%Viton), and has been developed rapidly in recent years. Charge density was set at 1.65 g·cm^{-3} by positioning pressing method and charge diameters were individually 1.5, 2, 3, 4, and 5 mm. At the same time, in order to avoid the charge height's potential influence on the output pressure, the experimental conditions were set at a charge height of 38 mm and a charge diameter of 20 mm, in a 45# steel charge sleeve. The manganin piezo-resistive sensor used in the experiment had dimensions of 0.254×0.127×0.01 mm, and with a 1-mm-thick organic glass sheet as the protective medium for the sensor and a 10-mm-thick organic glass protective block for the explosion container base.

3 Numerical Simulation

3.1 Physical model

AUTODYN numerical simulation software is commonly used in the field of highly dynamic process, and is especially suitable for the calculation of explosion and impact problems [7]. In the work reported here, the multi-material arbitrary Lagrangian-Eulerian (ALE) coupling algorithm by the AUTODYN software was applied to simulate the detonation growth and energy transfer process of a small-sized JO-9c explosive shown in Figure 2. A two-dimensional axisymmetric model was adopted in the calculation, with a small-sized charge of HMX in place of the miniature detonator to initiate the JO-9c explosive. For the convenience of comparison with the experimental results, the first grid node at the bottom of the small-sized charge was set as an observation point to record the shock wave pressure.

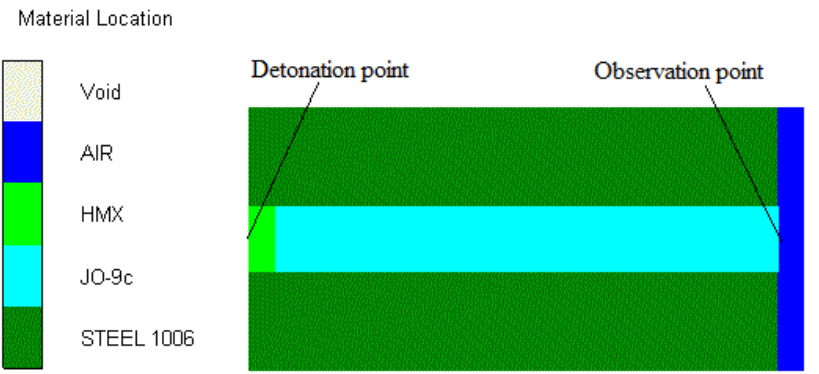

Figure 2. Simulation model for the AUTODYN software.

3.2 Material model

The materials considered in the work reported here include the initiating explosive, JO-9c explosive, the constraint shell and air. Only with the correct material model can the credibility of the results be guaranteed, therefore the choice of material model is crucial.

In the computation, HMX as an output charge of miniature detonator is merely used for blasting charges; therefore the detonation reaction process is normally ignored, and the expansion process of explosive products is commonly described by the JWL state equation, whose values can be checked in the AUTODYN material database [7].

For the constraint shell, in order to accurately describe the material state

under high pressure conditions, the shock state equation was used and the Gruneisen coefficient for the steel material is 2.17; then c_0 is 0.4569 cm·μs^{-1} and s is 1.49 [8].

Table 1. JO-9c parameters for ignition and growth reaction rate

I, [μs^{-1}]	b	a	m	G_1	c
7.43×10^{11}	0.667	0	20	3.1	0.667
d	y	G_2	e	g	z
0.111	1.0	400	0.333	1.0	2.0

The air filling the Euler grid was described by the ideal gas state equation, with an initial density of 0.001225 g·cm^{-3} and an initial pressure as standard atmospheric pressure.

For small-sized JO-9c explosives, the detonation wave propagation process can be affected by the lateral rarefaction wave due to the small charge diameter; therefore the small charge of JO-9c has properties typical of non-ideal detonation. To accurately describe the impact initiation and detonation process, it is necessary to introduce the trinomial ignition and growth model to describe the explosive reaction process in the reaction zone [9]:

$$\frac{dF}{dt} = I(1-F)^b\left(\frac{\rho}{\rho_0}-1-\alpha\right)^x + G_1(1-F)^c F^d P^y + G_2(1-F)^e F^g P^z \tag{3}$$

In this formula, F is the explosive reaction degree, assigned values between 0 to 1, with no explosive reaction indicated by $F=0$ and complete explosive reaction indicated by $F=1$; t is time; ρ is density; ρ_0 is the initial density; I, $G1$, $G2$, a, b, x, c, d, y, e, g, and z are all constants. The composition ratio of the JO-9c charge used in these experiments was the same as PBXN-5, and the parameters of the state equation can be checked in the AUTODYN material database. In addition, the parameters of the reaction rate equation are listed in Table 1 [10].

4 Results and Discussion

The manganin piezo-resistive sensor was used to test the output pressure for different charge diameters. Figure 3 illustrates a typical test signal, with point b as the time that the pulse of the constant current source applies a voltage to the sensor, while point d represents the time that the shock wave front reaches the sensor, U is the initial voltage at both ends of the sensor, and ΔU is the sensor

voltage change caused by the shock wave pressure acting on the sensor and the subsequent resistance change. When the detonation wave is conveyed to the sensor, the sensor signal first appears as a nearly linear voltage jump; this is the piezoresistive signal. The shock wave pressure can be obtained from the sensor calibration formula using the values of ΔU and U. Then the tensile deformation of the sensor, along with the superposition of the piezo-resistive signals and the tensile signals, occur under the action of the non-planar wave, until the sensor becomes short-circuited or open-circuited.

Table 2. The pressure results by experiment and numerical simulation with 45# steel constraint conditions

Number	Charge diameter [mm]	Quantity	Experimental pressure [GPa]	Correction pressure [GPa]	Simulation pressure [GPa]	Deviation [%]
1	1.5	10	9.090	15.33	17.50	14.15
2	2	10	12.229	18.87	20.26	7.37
3	3	9	16.359	22.25	22.61	1.62
4	4	10	18.304	22.98	22.29	-3.00
5	5	11	20.580	24.57	24.66	0.37
6	6	——	——	——	26.52	——
7	7	——	——	——	26.12	——
8	8	——	——	——	27.14	——

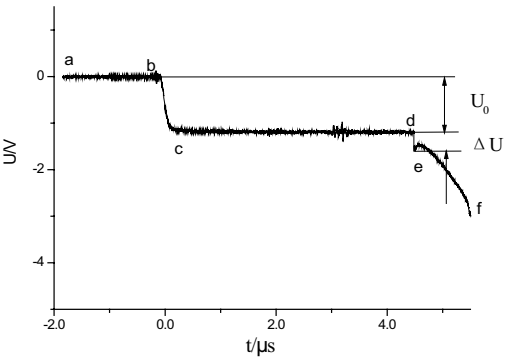

Figure 3. Typical test signal of a manganin piezo-resistive sensor.

The detonation growth process of a small-sized JO-9c explosive with different charge heights was simulated by the AUTODYN software. Figure 4

shows a typical pressure curve obtained from a numerical simulation. It can be seen that the pressure at the observation point near the end of the charge has a sudden increase resulting from the shock wave reaching this point. Then the shock wave pressure continues to propagate forwards, resulting in a pressure decrease. The highest point of the curve is the shock wave pressure value.

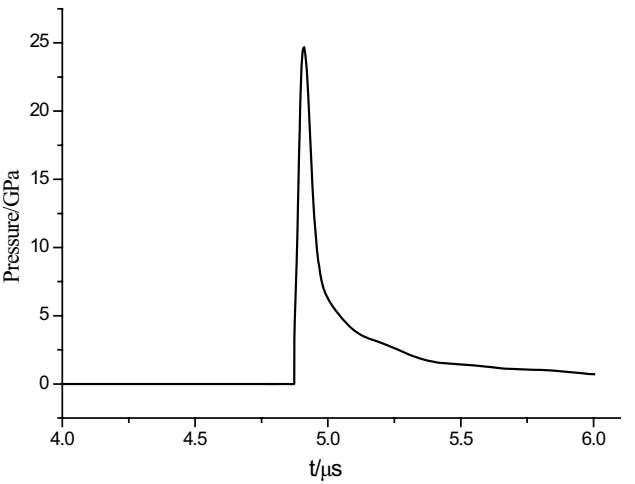

Figure 4. Simulation curve of a typical pressure/time plot.

In the numerical simulations, a number of observation points were set in the internal explosive charge in the central axis; Figure 5 shows the detonation pressure for a 5 mm charge diameter at different distances from the top. As shown in the curves, a small charge explosive has a detonation growth process, when the pressure gradually increases to a stable value for approximately 7.5 mm charge height, and basically remains unchanged thereafter. While the charge height in the experiment was set at 38 mm, which confirms that the value is adequate to guarantee complete detonation growth of the small charge and to reach steady detonation. It is remarkable that Figure 4 shows 25 GPa as the maximum pressure, while Figure 5 shows that the maximum pressure reaches 50 GPa. The reason for this difference is that the locations of the observation points in Figures 4 and 5 are not the same. Specifically, the observation point was designated as the first air grid node at the bottom of the small-sized charge in Figure 4 and in the internal explosive charge in Figure 5. Hence, the pressure obtained in Figure 4 is the output pressure of a small-sized charge, and the maximum pressure in Figure 5 is the Von Neumann spike of a small-sized charge detonation.

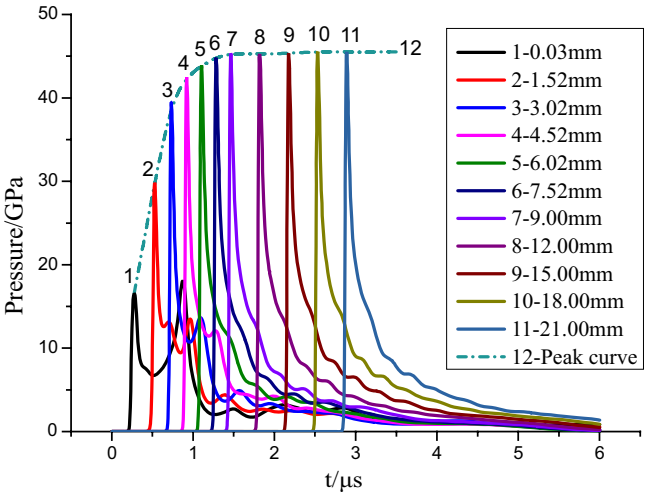

Figure 5. The pressure curves for a 5 mm charge diameter at different distances from the top.

Figure 6 shows the pressure contours for small charge detonation processes, from which it is clear that the explosive at the edge is affected by the lateral rarefaction wave and leads to detonation wave front bending. The radius of curvature of the wave front increases as the detonation wave propagates, but tends to become gradually stable, and finally remains constant. When the detonation waves reaches the terminus of the explosive pellet and is exposed to air, due to the large difference in shock wave impedance between air and explosive, the detonation wave decreases sharply on entering the air and turns into a shock wave.

Table 2 gives a comparison of numerical simulation results and experimental values. It is clear that the deviation between calculated results and experimental results increases with the decrease in charge diameter. This is because the explosive parameters used in the numerical simulations were measured using normal charge diameters; being applied to a small charge detonation will certainly introduce deviations. In general, a deviation less than 15% between numerical simulation results and experimental values indicates that the numerical simulation method for calculating the small charge detonation process has a definite reference value. By fitting the relation between charge diameter and output pressure obtained by experiment and numerical simulation, the curve shown in Figure 7 was obtained. From this fitting curve, the detonation output pressure of a small diameter explosive pellet increases with charge diameter, but the trend becomes slower, and eventually achieves a steady detonation output pressure. According to the measured fitting curve, a small charge size, within 1.5~3 mm, exhibits the

largest increase; for instance, the detonation pressure value for a 3 mm charge diameter is 43.27% higher than that for a 1.5 mm charge diameter. That is to say, the smaller the charge diameter is, the faster the pressure value decreases with charge diameter. This means that the change in pressure value is more dependent on the charge size, and an abrupt change in rate occurs for 3 mm charge diameter. According to the above analysis, it is necessary to increase the charge diameter to get close to the limiting diameter in the choice of small-sized charges.

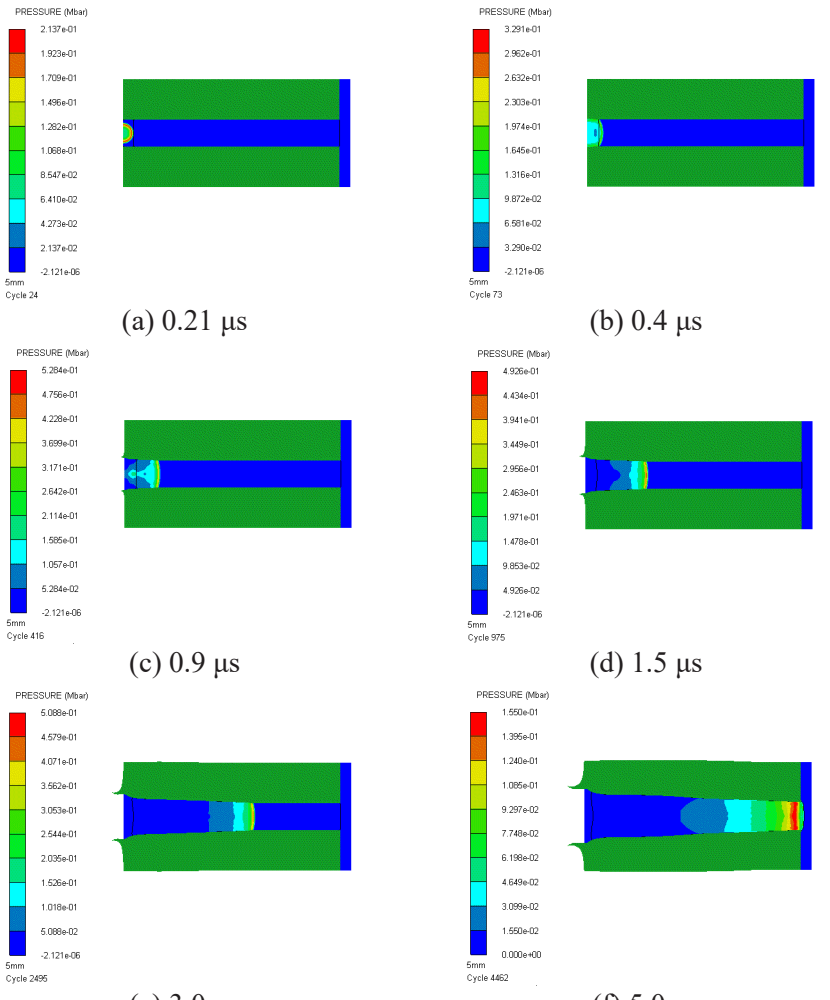

Figure 6. The pressure contours for small charge detonation processes.

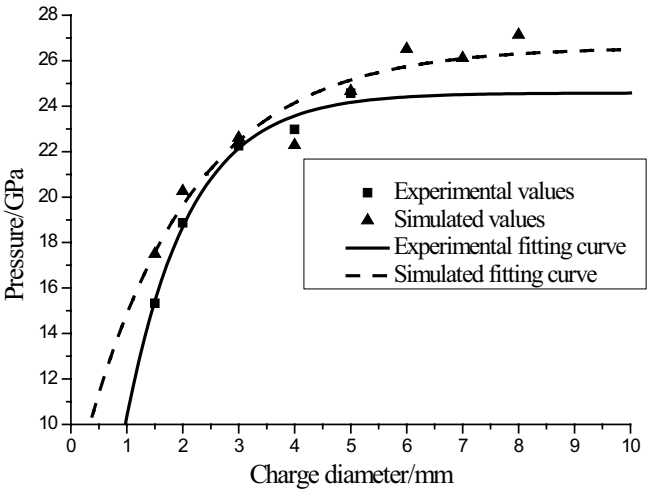

Figure 7. The fitting curves for detonation pressure versus charge diameter.

The experimental data fitting curve was: $P = 24.578 - 9.213e^{\frac{1.493-d}{1.132}}$, with a correlation coefficient of 0.958.

The simulation data fitting curve was: $P = 26.601 - 9.332e^{\frac{1.439-d}{1.914}}$, with a correlation coefficient of 0.904.

Non-ideal detonation causes the influence of a small charge diameter on the output pressure. When the detonation wave propagates along the explosive pellet with certain charge diameters, the detonation products expand laterally at the same time. The lateral sparse wave, caused by the lateral expansion, can gather along the axial direction at the local velocity of sound. The smaller the charge diameter is, the shorter is the convergence time, and the faster the detonation pressure decreases in the reaction zone. When the charge diameter is less than the critical diameter, energy dissipation caused by the lateral rarefaction wave is extremely large, resulting in the surplus energy being insufficient to stimulate explosive detonation of the next level, and detonation is finally quenched. From the fitting formula obtained, the detonation pressure value of small charge explosives is basically stable if the charge diameter is over 5 mm, and the explosive detonation pressure value for a 5.1 mm charge diameter is merely 0.09% higher than that for 5 mm, while the explosive detonation pressure for a 6 mm charge diameter is 0.03% higher than that for 5 mm; therefore the JO-9c limiting charge diameter is evaluated as 5 mm. From the experimental fitting formula, it can be calculated that when the pressure is zero, the charge diameter

is about 0.34 mm. By this stage it would inevitably be difficult for the charge to maintain a steady detonation; hence, 0.34 mm can be used as the critical diameter of JO-9c, which is also consistent with data reported in the literature [11].

5 Conclusions

(1) The charge diameter of JO-9c has significant influences on the explosive output pressure. The output pressure of a small diameter explosive pellet increases with charge diameter and tends to gradually achieve a steady detonation output pressure. The smaller the charge diameter is, the faster the pressure value decreases with charge diameter; in other words, the pressure change is more dependent upon the charge size, and an abrupt change in rate occurs when the charge diameter exceeds 3 mm.

(2) The output pressure of small charge explosives is basically stable with charge diameters over 5 mm, with the pressure value for a 6 mm charge diameter merely 0.03% higher than that for 5 mm charge; therefore for JO-9c, the limiting charge diameter is evaluated as 5 mm. When the pressure is zero, the charge diameter is calculated to be approximately 0.34 mm. By this stage it would inevitably be difficult for the charge to maintain a steady detonation; hence, 0.34 mm can be used as the critical diameter of JO-9c.

(3) With the established numerical calculation model of small charge explosives, the numerical simulation method can be used to predict the detonation pressure and the detonation growth process with 15% uncertainty with respect to experimental values measured by the manganin piezo-resistance test method.

6 References

[1] Pezous H., Rossi C., Sanchez M., Mathieu F., Dollat X., Charlot S., Salvagnac L., Conédéra V., Integration of a MEMS Based Safe Arm and Fire Device, *Sens. Actuators, A*, **2010**, *159*(2), 157-167.

[2] Robinson C.H., Wood R.H., Gelak M.R., Hollingsworth H., *Micro-scale Firetrain for Ultra-miniature Electro-mechanical Safety and Arming Device*, US Patent 7069861 B1, **2006**.

[3] Sun C. W., Zhao F., Gao W., A Detonation Shock Dynamics Approach to the Diameter Effect of Explosive Sticks (in Chinese), *Baozha Yu Chongji*, **1996**, *16*(3), 193-200.

[4] Wang B., Tan D.W., Zhao J.B., Wen S.G., Diameter Effect of JBO-9021 Rate Sticks

at Room Temperature (in Chinese), *Baozha Yu Chongji*, **2012**, *32*(5), 490-494.
[5] Xiao D.J., Pu C.J., Experimental Study Diameter Effect of Explosive Speed (in Chinese), *Xiandai Kuangye*, **2011**, *501*(1), 30-33.
[6] Xu X.C., Jiao Q.J., Cao X., Attenuation Regularity of Detonation Wave of Small Charge in PMMA (in Chinese), *Hanneng Cailiao*, **2009**, *17*(4), 431-435.
[7] Shi S.Q., Wang M., Sun B., Fang X.W., Liu Y.F., *AUTODYN Engineering Dynamic Analysis and Application Examples* (in Chinese), Vol. 1, China Architecture & Building Press, Beijing, **2011**; ISBN 9787112138005.
[8] Zhang B.P., Zhang Q.M., Huang F.L., *Detonation Physics* (in Chinese), Vol. 1, Weapon Industry Press, Beijing, **2001**, pp. 444-445; ISBN 7801329864.
[9] Lee E.L., Travel C.M., Phenomenological Model of Shock Initiation in Heterogeneous Explosives, *Phys. Fluids*, **1980**, *12*(23), 2362-2372.
[10] Cao X., *Study on the Structure of High-effect-booster Charge and Numerical Simulation on its Initiation Process* (in Chinese), North University of China, China, **2005**.
[11] Li X.G., *Study on the Technique of Explosive Logic Circuit of Optional Output* (in Chinese), Beijing Institute of Technology, China, **2009**.